Plant Physiology Preview. Published on July 1, 2016, as DOI:10.1104/pp.16.01028

Isolation of mesophyll specialized cells by FACS

***Corresponding Author**
Mariana Sottomayor
CIBIO/InBIO - Centro de Investigação em Biodiversidade e Recursos Genéticos
Universidade do Porto, Campus Agrário de Vairão
4485-661 Vairão, Portugal
e-mail: mssottom@fc.up.pt
Tel. + 351 22 0402820
Fax +351 252 661 780

Isolation of cells specialized in anticancer alkaloid metabolism by fluorescence activated cell sorting

Inês Carqueijeiro[§], Ana Luísa Guimarães[§], Sara Bettencourt, Teresa Martínez-Cortés, Joana G. Guedes, Rui Gardner, Telma Lopes, Cláudia Andrade, Cláudia Bispo, Nuno Pimpão Martins, Paula Andrade, Patrícia Valentão, Inês M. Valente, José A. Rodrigues, Patrícia Duarte, Mariana Sottomayor*

CIBIO/InBIO - Centro de Investigação em Biodiversidade e Recursos Genéticos Universidade do Porto, Campus Agrário de Vairão, 4485-661 Vairão, Portugal (S.B., T.M.C., J.G.G., M.S.); IBMC – Instituto de Biologia Molecular e Celular, Universidade do Porto, Rua do Campo Alegre, 823, 4150-180 Porto, Portugal (I.C., A.L.G., P.D.); Departamento de Biologia, Faculdade de Ciências da Universidade do Porto, Rua do Campo Alegre s/n 4169-007 Porto, Portugal (I.C., M.S.); ICBAS – Instituto de Ciências Biológicas Abel Salazar, Universidade do Porto, Rua de Jorge Viterbo Ferreira n.º 228, 4050-313 Porto, Portugal (J.G.G.); Instituto Gulbenkian de Ciência, Rua da Quinta Grande 6, 2780-156 Oeiras, Portugal (R.G., T.L., C.A., C.B., N.P.M.); REQUIMTE/Laboratório de Farmacognosia, Departamento de Química, Faculdade de Farmácia, Universidade do Porto, Rua de Jorge Viterbo Ferreira, n° 228, 4050-313 Porto, Portugal (P.A., P.V.); REQUIMTE/LAQV - Departamento de Química e Bioquímica, Faculdade de Ciências, Universidade do Porto, Rua do Campo Alegre, nº 687, 4169-007 Porto, Portugal (I.M.V., J.A.R.)

[§] These authors contributed equally to the article.

* Corresponding author

SUMMARY

Idioblasts from *Catharanthus roseus* leaves specifically accumulate alkaloids and show autofluorescence that enabled the fluorescence activated cell sorting of a population of idioblast protoplasts.

Author contributions

MS conceived research, supervised most experiments and designed and performed experiments; IC, ALG, SB, TMC, JGG, TL, CA, CB, NPM, IMV and PD designed and/or performed different sets of experiments; PA and PV provided technical assistance; RG and JAR supervised specific experiments; ALG prepared most of the figures; MS wrote the manuscript with contributions from all the authors.

Financial sources

This work was funded: i) by FEDER funds through the Operational Competitiveness Programme – COMPETE and by National Funds through FCT – Fundação para a Ciência e a Tecnologia under the projects FCOMP-01-0124-FEDER-037277 (Pest-C/SAU/LA0002/2013), FCOMP-01-0124-FEDER-019664 (PTDC/BIA-BCM/119718/2010) and FCOMP-01-0124-FEDER-028125 (PTDC/BBB-BIO/2231/2012); ii) by FEDER funds and FCT/MEC national funds, under the Partnership Agreement PT2020, within the project UID/ QUI/50006/2013 - POCI/01/0145/FERDER/007265; iii) by the FCT scholarships co-supported by FCT and the European Social Fund SFRH/BD/4190/2007 (IC), SFRH/BD/97590/2013 (JGG) and SFRH/BPD/111181/2015 (IMV); v) by a Scientific Mecenate Grant from Grupo Jerónimo Martins SA.

Present addresses

Inês Carqueijeiro

Université François-Rabelais de Tours

EA2106 Biomolécules et Biotechnologies Végétales

Département de Biologie et Physiologie Végétales

UFR Pharmacologie, Parc de Grandmont, 37200 Tours, France

Ana Luísa Guimarães

Berlin Institute for Medical Systems Biology

Max Delbrück Center for Molecular Medicine in the Helmholtz Association

Robert-Rössle-Straße 10

H. 89, Rm. 2.12

13125 Berlin, Germany

*__Corresponding Author__

Mariana Sottomayor

e-mail: mssottom@fc.up.pt

ABSTRACT

Plant specialized metabolism presents often a complex cell-specific compartmentation essential to accomplish the biosynthesis of valuable plant natural products. Hence, the disclosure and potential manipulation of such pathways may depend on the capacity to isolate and characterize specific cell types. *Catharanthus roseus* is the source of several medicinal terpenoid indole alkaloids, including the low-level anticancer vinblastine and vincristine, for which the late biosynthetic steps occur in specialized mesophyll cells called idioblasts. Here, the optical, fluorescence and alkaloid accumulating properties of *C. roseus* leaf idioblasts are characterized, and a methodology for the isolation of idioblast protoplasts by fluorescence activated cell sorting is established, taking advantage of the distinctive autofluorescence of these cells. This achievement represents a crucial step for the development of differential omic strategies leading to the identification of candidate genes putatively involved in the biosynthesis, pathway regulation and transmembrane transport leading to the anticancer alkaloids from *C. roseus*.

INTRODUCTION

Plants depict a unique metabolic plasticity including a wealth of natural products that help them to deal with a wide range of environmental threats. Many of those specialized metabolites have valuable applications as medicines, colorants, flavors, fragrances, etc., but their exploitation is often hindered by their low levels and limited availability of plant material. The intrinsic complexity of specialized pathways has been a major challenge to their full characterization, but it can now deliver potent tools, if combined with the recent development of omic technologies. Therefore, the association of differential omic screenings to the regulation of specialized pathways by environmental-developmental-cues, and to their organ- tissue-specific organization is enabling the fast disclosure of important parts of long time searched pathways (Miettinen et al., 2014; Stavrinides et al., 2015). However, there is a level of complexity that is particularly challenging concerning the application of these approaches - the expression of different parts of the pathway in specific cell types within a tissue or organ. The low relative abundance of those cell types within the respective plant organs hampers the retrieval of candidate genes but, if isolation of such cells is achieved, it constitutes a powerful tool. Two major techniques may be explored to this end: Laser Microdissection (LMD) and Fluorescence Activated Cell Sorting (FACS). The use of LMD for plant microsampling has increased significantly over the past decade (Fang and Schneider, 2014). FACS, however, in spite of being a method possibly more cost- and time-effective for obtaining samples with quantity and quality guaranteeing successful cellular ‘omics’, has been mostly applied to the sorting of protoplasts from Arabidopsis root and shoot apical cells specifically labeled with GFP (Birnbaum et al., 2005; Galbraith, 2010; Carter et al., 2013).

A paradigmatic example of cell-specific compartmentation involving autofluorescence is the terpenoid indole alkaloid (TIA) pathway in the medicinal plant *Catharanthus roseus* (Supplemental Fig. S1), whose leaves accumulate in low-levels the anticancer TIAs vinblastine (VLB) and vincristine (VCR) (De Luca et al., 2014). The TIA pathway presents multi-cellular compartmentation in *C. roseus* leaves, with early and middle steps being expressed in internal phloem associated parenchyma and the epidermis, whereas late steps are expressed in

laticifers and idioblas, characterized by a conspicuous fluorescence (St-Pierre et al., 1999; Courdavault et al., 2014). A diversity of *C. roseus* transcriptomic projects (MPGR, Phytometasyn, Cathacyc) has enabled a recent burst of research in the TIA pathway, leading to the full characterization of its iridoid / terpenoid precursor part, of late biosynthetic steps, and of the first TIA transporter (Yu and DeLuca, 2013; Miettinen et al., 2014; Stavrinides et al. 2015; Kellner et al., 2015,). However, the last bottleneck part of the pathway leading to the anticancer alkaloids remains elusive, as well as most TIA transmembrane transporters and transcriptional regulators affecting VLB / VCR levels.

This study describes the distinctive properties of *C. roseus* leaf idioblasts and the optimization of FACS conditions allowing the successful separation of idioblast protoplasts from those of common mesophyll cells. The amount / quality of cells sorted and the buffer composition makes the sorting methodology developed here compatible with the implementation of subsequent transcriptomic, metabolomic and proteomic studies, crucial to fully unravel the TIA pathway.

RESULTS AND DISCUSSION

Idioblasts and laticifers from *C. roseus* leaves are differentially stained by alkaloid indicators and depict a characteristic autofluorescence

Infiltration of leaves with both the reagent of Dragendorff and the reagent of Mayer, widely used to identify alkaloids, characteristically labeled a particular set of cells with distinct scattered patterns in the adaxial and abaxial sides of the leaves, previously identified as idioblasts (Fig. 1; Yoder and Mahlberg, 1976; Mersey and Cutler, 1986; St-Pierre et al., 1999). Labeling was also associated with small veins, likely corresponding to reaction with alkaloids accumulated in the unbranched, nonarticulated laticifers described by Yoder and Mahlberg (1976). Focusing of different planes of the leaf surface enabled to conclude that the epidermal cells did not react with the reagents and that the two different abaxial/adaxial patterns of idioblasts likely corresponded to the spatial organization of such cells in the two respective underlying tissues, the

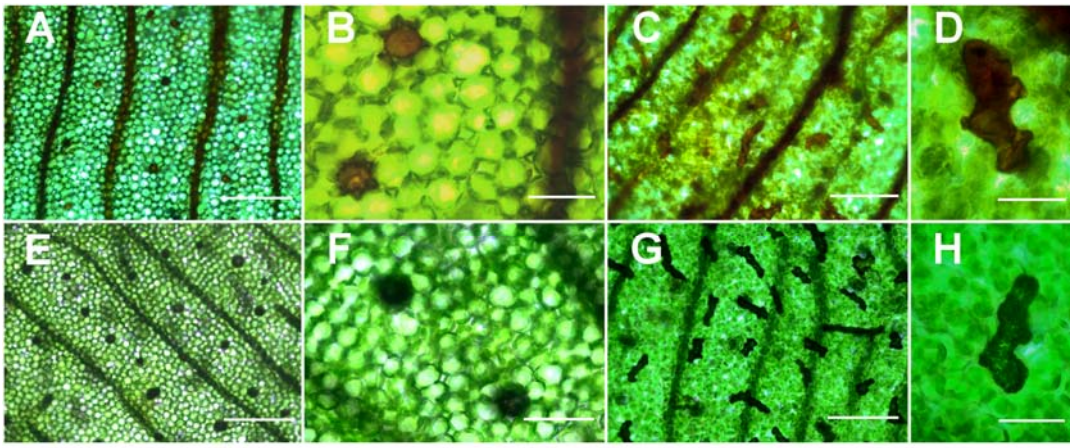

Figure 1. Bright-field optical microscopy images of *C. roseus* whole leaves infiltrated with alkaloid indicators reveal a positive reaction in idioblasts (stained isolated mesophyll cells) and laticifers (stained threads). A to D, Infiltration with the reagent of Dragendorff reveals alkaloid accumulating cells stained in brown. E to H, Infiltration with the reagent of Mayer reveals alkaloid accumulating cells stained in dark grey. A, B, E and F, Images of the adaxial face. C, D, G and H, Images of the abaxial face. Focusing of leaf images was performed based on the detection of stained cells, which appeared only below the epidermis cell layer. Bars = 200 µm (A, C, E and G) and 50 µm (B, D, F and H).

spongy and the palisade parenchymas, as could also be concluded from the shape of the cells (Fig. 1 B, D, F, H). This differential accumulation of alkaloids in laticifers and idioblasts of *C. roseus* leaves was previously reported by Yoder and Mahberg (1976) and is also supported by the work of Mersey and Cutler (1986), who detected a higher level of TIAs in cell fractions enriched in idioblast protoplasts. Therefore, our results confirm the importance of idioblasts as alkaloid accumulation targets, with their accumulation capacity likely influencing the whole metabolic flux of the pathway. As such, idioblasts are certainly home of key alkaloid transporters and possibly also of some key biosynthetic steps, as already shown by St-Pierre et al. (1999).

Under the fluorescence microscope, the exact same pattern of cells reacting with alkaloid indicators depicted a distinctive vacuolar autofluorescence characterized by blue and green emissions upon UV excitation (Fig. 2). The strong autofluorescence of idioblasts observed in this study was also previously reported, albeit with somewhat different emission profiles (Mersey and Cutler 1986; St-Pierre et al. 1999). Considering the fluorescence excitation and emission spectra of the main *C. roseus* TIAs determined by Renaudin (1985), only the TIA serpentine may be partially contributing to the blue autofluorescence observed in this study, with the bulk of the autofluorescence signal, namely in the green spectrum, being due to unknown compounds.

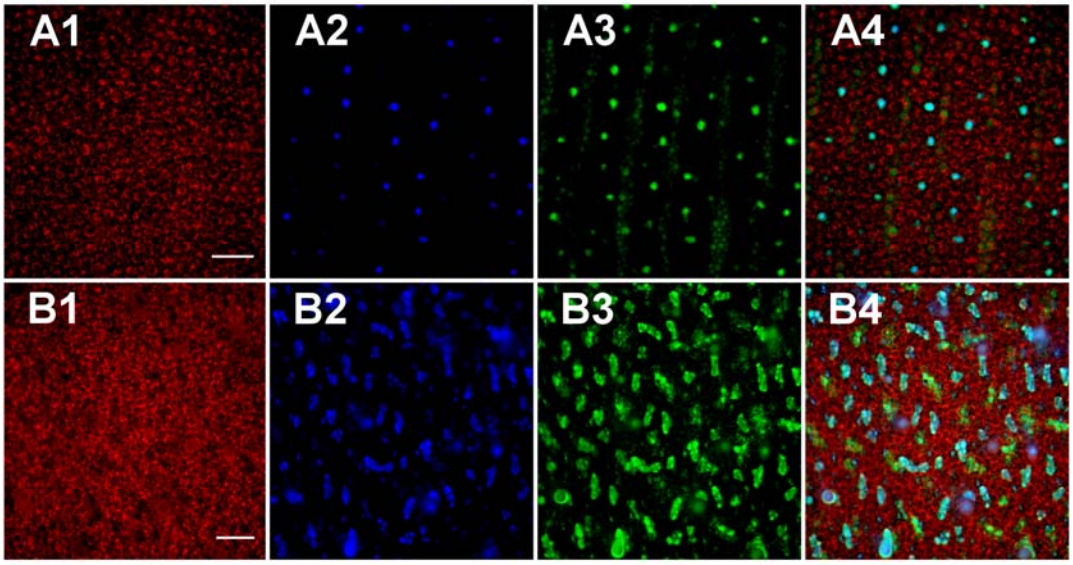

Figure 2. Epifluorescence microscopy images of *C. roseus* whole leaves. A, Image of the adaxial face. B, Image of the abaxial face. 1, Red channel revealing autofluorescence of chlorophyll in chloroplasts. 2, Blue channel revealing the presence of an autofluorescence signal in idioblasts. 3, Green channel revealing the presence of an autofluorescence signal in idioblasts. 4, Merged images of the three channels. Bars = 100 µm.

Overall, these results indicated the presence in *C. roseus* leaves of cells specifically accumulating alkaloids and depicting a distinctive autofluorescence that makes them potentially amenable to FACS approaches.

FACS allows the isolation of a highly enriched population of *C. roseus* leaf idioblasts suitable for differential omic screenings

In order to make possible the sorting of the fluorescent idioblasts, the cell wall of *C. roseus* leaves was digested with an optimized protocol that enabled the production of a high yield of pure and stable protoplasts (Fig. 3A). Treatment with the reagents of Mayer and Dragendorff indicated that idioblast protoplasts retained their distinctive capacity to accumulate alkaloids (Fig. 3, B and C). Furthermore, it was possible to observe that those reagents stained specifically the vacuole, where alkaloids are known to accumulate. Interestingly, under the bright-field microscope and when focused above their mid-plane, idioblasts presented a distinctive bright halo, likely resulting from a higher refraction index of the vacuole content (Fig. 3, D and E). This further indicated a distinct chemical composition of idioblasts, at the same time it provided a way to identify them under the bright-field microscope. Upon UV excitation, idioblast protoplasts showed intense blue and green fluorescence,

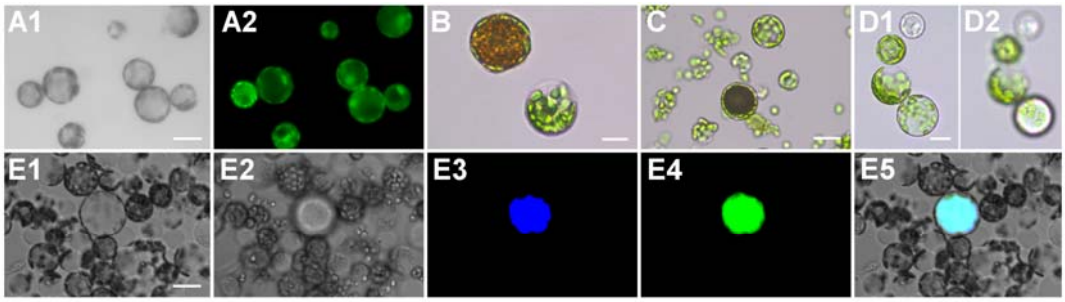

Figure 3. A, Bright-field image (A1) of *C. roseus* leaf protoplasts and the correspondent fluorescence image showing the viable protoplasts that incorporated and modified FDA to generate green fluorescence (A2). B, Bright-field image of protoplasts treated with the reagent of Dragendorff showing an idioblast with the vacuole content stained in brown. C, Bright-field image of protoplasts treated with the reagent of Mayer showing an idioblast with the vacuole content stained in dark grey (many protoplasts burst in the presence of this reagent). D, Bright-field image of protoplasts focused at the mid-plane (D1) and above the mid-plane (D2) showing an idioblast with a distinctive bright halo. E, Bright-field and epifluorescence microscopy images of leaf protoplasts with cells: focused at the mid plane (E1), focused above the mid plane showing that idioblasts display a distinctive bright halo (E2), observed with the blue channel revealing idioblast protoplasts (E3), observed with the green channel revealing idioblast protoplasts (E4), and represented by the merged image of E1, E3 and E4 (E5). Bars = 10 µm (A, B and D) and 20 µm (C and E).

indicating they also retained the original fluorescence properties (Fig. 3 E). In fact, the emission spectra of these cells were highly similar to the emission spectra of the leaf idioblasts, and markedly different from other mesophyll leaf cells, or from other protoplasts (Fig. 4), clearly confirming the identity of the fluorescent, refractive protoplasts as idioblasts. Overall, it was clear that idioblast protoplasts retained their original distinctive chemical composition and identity, and therefore constituted highly interesting targets for cell sorting and differential characterization.

To sort *C. roseus* protoplasts relying on their intrinsic fluorescence properties, the PMT (photomultiplier tube) detector voltages of the sorter were set to maximize differences between the minimum and maximum fluorescence for the blue, the green, and the red channels. PBS worked well as sheath buffer for sorting of the *C. roseus* protoplasts, but it lowered the stability of the sorted cell populations in comparison with the use of protoplast suspension buffer as sheath. Therefore PBS should be used only when further manipulation of cells is not needed, such as for metabolomic or transcriptomic studies.

Analysis of the sorted events using all the different combinations of fluorescence signals in two and three dimension dot plots revealed that the combination of the red and green signals depicted in Fig. 5A was the one giving a better definition of the different cell populations. Sorted cells from all over the

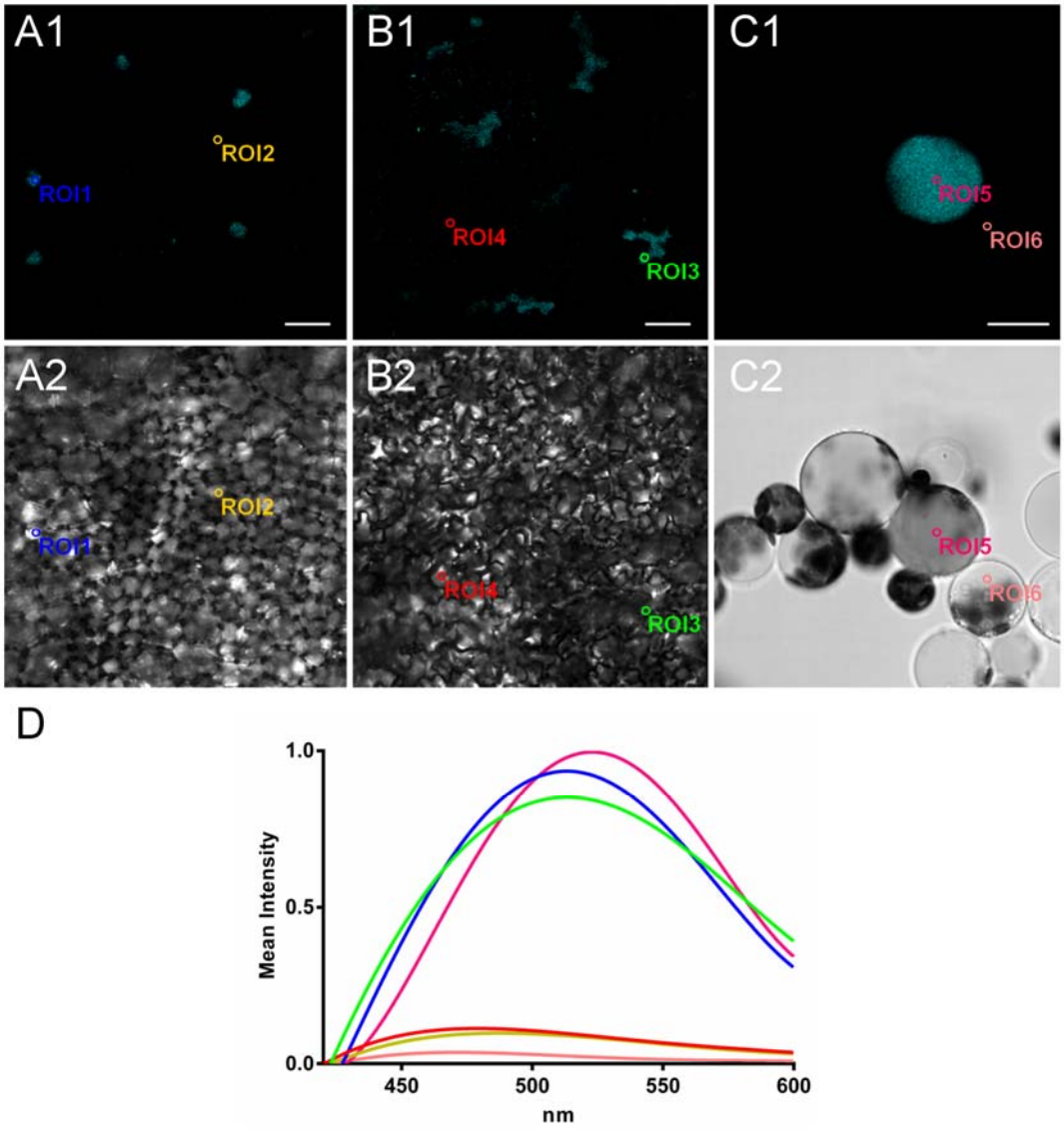

Figure 4. Autofluorescence emission spectra of *C. roseus* mesophyll cells. A, Confocal (A1) and bright-field (A2) images of the adaxial face of a whole mounted leaf focused at the level of the palisade parenchyma. B, Confocal (B1) and bright-field (B2) images of the abaxial face of a whole mounted leaf focused at the level of the spongy parenchyma. C, Confocal (C1) and bright-field (C2) images of mesophyll protoplasts. D, Emission spectra of the cells indicated in A, B and C. upon excitation with a 405 nm laser. Bars = 50 µm (A and B) and 20 µm (C).

spectrum of events detected were collected in MM buffer and were observed under the fluorescence microscope. This enabled to identify populations I and II as targets (Fig. 5A): population I was constituted exclusively by cells with a high number of chloroplasts, with low blue/green autofluorescence and low refraction of the vacuolar content, clearly enabling their identification as a pure population of common mesophyll cells (Fig. 6, B and C); population II was constituted by 90% of cells depicting an intense blue/green autofluorescence and a high refraction of the vacuolar content, enabling their identification as idioblasts (Fig.

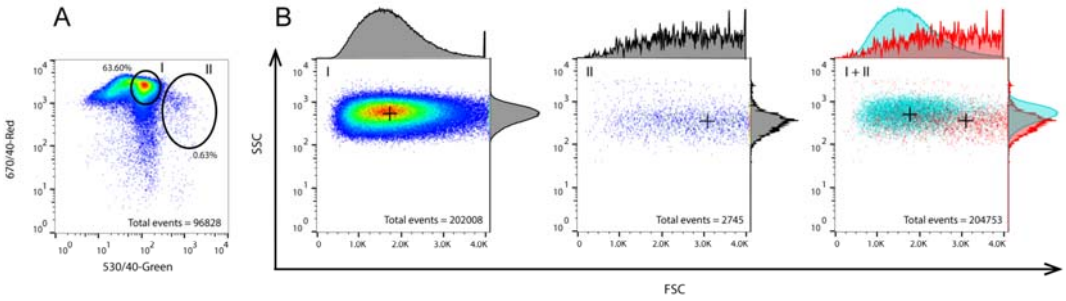

Figure 5. Dot plots obtained during sorting of *C. roseus* leaf protoplasts. A, Dot plot of red versus green emissions with indication of the two populations selected as common mesophyll cells (I) and idioblasts (II), based on bright field and fluorescence microscopy of the sorted cells (Fig. 6). Events corresponding to debris were excluded from the dot plot. B, Dot plots of forward scatter (FSC) vs. side scatter (SSC) of the two populations highlighted in A. Crosses indicate medians of populations in both FSC and SSC.

6, D and E). When comparing the forward (FSC) and side (SSC) scatter properties of the two populations (Fig. 5B), it was observed that they overlap partially, with population II (idioblasts) having an average higher FSC and lower SSC, but with a high heterogeneity of values. Since FSC increases with particle refraction index and size, and SSC increases with granularity or higher amount of cellular components, these results match microscope observations of idioblasts, which show a higher refraction index and often a big cell size, although with a high heterogeneity in size (Fig. 3, D and E, and Fig. 6A). In average it was possible to sort and recover ~ 50,000 cells of population II (idioblasts) per operation day, and tens fold more of common mesophyll cells.

To test the feasibility of using the sorted cells for transcriptomic studies, the sorted cells were collected directly to RNA extraction buffer and their RNA was isolated, with about 50,000 cells yielding 200 ng of RNA for the two sorted populations, as well as for the whole protoplast mother suspension, all with high quality (RNA quality indicator/RQI ≥ 8). qPCR analysis of the genes involved in the late steps of TIA biosynthesis desacetoxyvindoline 4-hydroxylase (D4H) and deacetylvindoline 4-O-acetyltransferase (DAT) further confirmed the suitability of the sorted cells for transcriptomic studies, and showed a ~3 fold increase in the transcript levels of those genes in idioblasts, in line with previous in situ hybridization studies of these two genes (Fig. 7; St-Pierre et al. 1999).

In order to demonstrate that the sorted cells may also be used for metabolomic studies, namely in what concerns alkaloid profile, methanolic extracts obtained from roughly 200.000 sorted common mesophyll cells and ~ 25,000 sorted idioblasts were analyzed by LC-MS/MS. Fig. 8 shows the easy

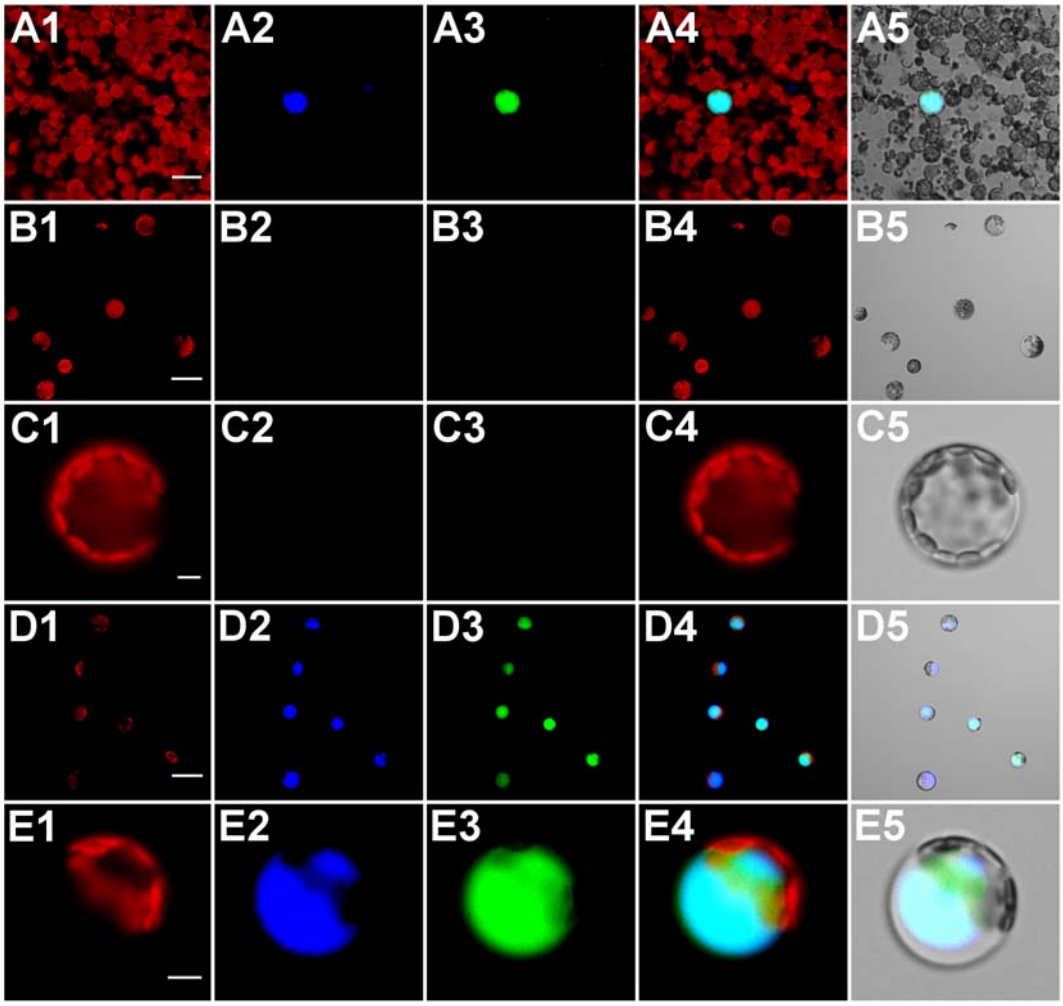

Figure 6. Epifluorescence microscopy images of a source C. roseus leaf protoplast suspension (A) and of populations of mesophyll cells (B and C) and idioblasts (D and E) isolated by FACS. 1, Red channel revealing autofluorescence of chlorophyll in chloroplasts. 2, Blue channel revealing the presence of an autofluorescence signal in idioblasts. 3, Green channel revealing the presence of an autofluorescence signal in idioblasts. 4, Merged images of the three channels. 5, Merge of the blue and green channel images with the correspondent bright-field image. Bars = 40 µm (A, B and D) and 5 µm (C and E).

detection of the leaf abundant VLB monomeric precursor vindoline (Carqueijeiro et al. 2013) in sorted common mesophyll cells and idioblasts. The results confirm that idioblasts are impressive TIA accumulation targets, showing levels of vindoline ~3,000 fold higher than common mesophyll cells (315.22 ng per idioblast versus 0.105 ng per mesophyll cell).

In conclusion, the mesophyll of *C. roseus* leaves presents scattered idioblasts that specifically accumulate high levels of alkaloids and depict a distinctive conspicuous autofluorescence, which allows the isolation of idioblast protoplasts retaining their original identity by means of an optimized FACS method. The procedure enables the isolation of a high number of cells, 50,000

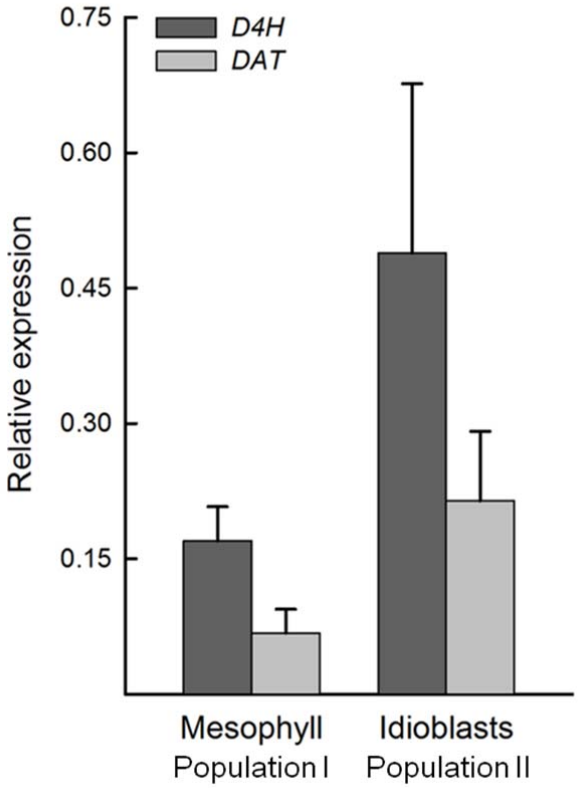

Figure 7. Expression of *D4H* and *DAT* in sorted common mesophyll and idioblast protoplasts. Transcript levels were determined by qPCR and normalized using Cr*RPSL24* ($p<0.05$ for both genes, Student's t-test).

idioblast cells per operation day (from *ca.* 3.5 g of leaves), easily reaching 250,000 upon 5 days of work, highly exceeding the total 2,500-5,000 idioblast cells isolated by Murata and De Luca (2005) using LCM. The idioblast cell fraction obtained in this study is highly enriched, and is now being used for the implementation of differential transcriptomic and metabolomic studies to uncover the differentiation status and functions of idioblasts, as well as novel candidate genes potentially involved in key events of the biosynthesis, transport and regulation of the medicinal TIA pathway.

MATERIAL AND METHODS

Plant material

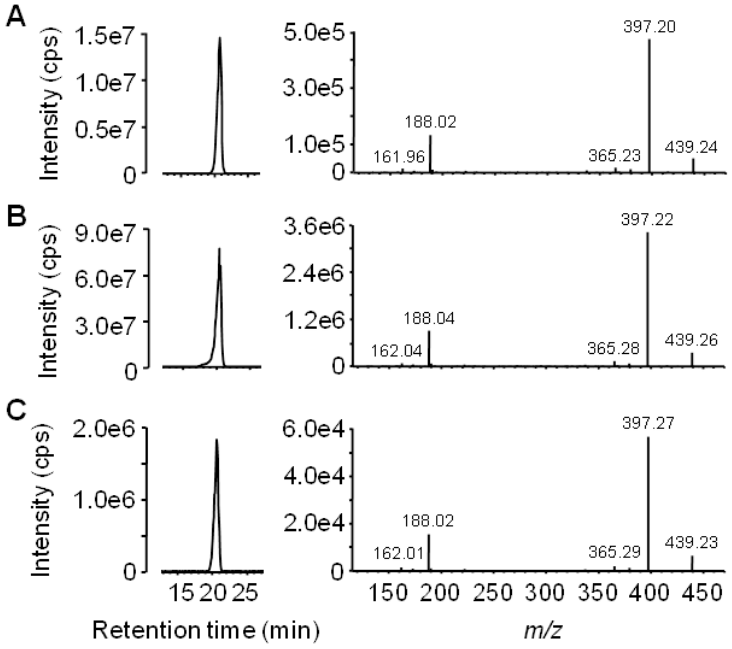

Figure 8. Base peak chromatogram of *m/z* 457.23 and respective MS fragment pattern. A, Vindoline standard (0.5 µg mL^{-1}). B, Sorted idioblast protoplasts (115 cells $µL^{-1}$). C, Sorted common mesophyll protoplasts (800 cells $µL^{-1}$).

Catharanthus roseus (L.) G. Don cv. Little Bright Eye plants were grown at 25 °C, in a growth chamber, under a 16/8 hr photoperiod, using white fluorescent light with a maximum intensity of 70 µmol m^{-2} s^{-1}. Seeds were acquired from B&T World Seeds (Aigues-Vives, France). Plants used for protoplast isolation were 6 to 8 months old.

Alkaloid indicators

The reagents of Dragendorff and Mayer were prepared as described in Bruneton (2009). Both reagents were diluted 1:10 with water just before use. For detection of alkaloids in leaves, the reagents were infiltrated through the abaxial face of a whole leaf using a syringe without needle. For alkaloid detection in protoplasts, a small drop of diluted reagent was added to an excess of protoplast suspension.

Isolation and characterization of *C. roseus* leaf protoplasts

The isolation of leaf protoplasts was performed as described in Carqueijeiro et al. (2013). Protoplasts were diluted in MM buffer to $5x10^5$ to $2x10^6$ cells mL^{-1},

and observed using an optical microscope (Olympus, Japan) with a coupled Olympus DP 25 Digital Camera and Cell B software. Protoplasts were also observed using a Leica DMI6000 microscope body equipped with a Hamamatsu Flash Orca 4.0 LT sCMOS camera with 10x Plan Fluor 0.3 NA and 20x Plan Apochromat 0.7 NA objectives controlled through the Leica LAS X software (Leica Microsystems, Germany). For acquisition of blue and green autofluorescence, the excitation band pass filter was 350/50 nm, associated to an emission filter of 455/50 nm (blue) and of 525/36 nm (green). For acquisition of red autofluorescence, the excitation was 490/20 nm and emission was 705/72 nm.

Viability of protoplasts was assayed as described in Carqueijeiro et al. (2013). Autofluorescence characterization of protoplasts was performed in a confocal microscope Leica TCS SP5 II (Leica Microsystems, Germany) controlled through the Leica LAS 2.6 software, using the diode 405 nm laser to excite and recording a spectral series from 420 to 600 nm, with a detection band width of 5 nm.

Fluorescence Activated Cell Sorting (FACS) of *C. roseus* protoplasts

Leaf protoplasts suspended in MM buffer were run in a MoFlo (Beckman Coulter, Fort Collins, USA), at 4 ºC, immediately after isolation. The protoplast suspension was carefully homogenized immediately prior to use and whenever needed during the sorting. Protoplasts were sorted using either protoplast isolation medium or PBS as sheath, at a constant pressure of 200 kPa (~30 psi), using a 100 µm nozzle and a drop drive frequency of ~40 kHz (~40,000 drops / sec). The total event rate was kept below 8,000 events / sec. Autofluorescence was detected using a water-cooled I90-C Coherent argon laser operating at multiline UV wavelengths (330-360 nm) with 50 mW output as excitation source, and two different emission band-pass filters, 455/30 nm and 530/40 nm for blue and green fluorescent detection, respectively. Scatter measurements were carried out at 488 nm using a Coherent Sapphire 488-200 CDRH laser, with 140 mW output, which was also used for detection of chlorophyll autofluorescence together with a 670/40 nm band-pass emission filter. Sorted cells were collected in microcentrifuge tubes containing a buffer adapted to subsequent processing. For imaging, 200 cells were sorted onto a

slide containing 10 µl of protoplast isolation medium and immediately observed in the Leica High Content Screening microscope as described above.

RNA extraction and cDNA synthesis

RNA was isolated using the RNeasy Plant Mini kit (Qiagen, Limburg, Netherlands) according to the manufacturer's instructions with the modifications described by Birnbaum et al. (2005). RNA quantity and quality assessment was performed in EXPERION™ Automated Electrophoresis System (Bio-Rad, Hercules, CA, USA). For the synthesis of cDNA, 150 ng of the isolated RNA was treated with DNaseI (Thermo Scientific), followed by enzyme inactivation by heating at 65 °C for 10 min in the presence of 20 mM EDTA. First-strand cDNA was synthesized from total RNA using the iScript™ cDNA Synthesis Kit (BioRad) and oligo (dT) according to manufacturer's instructions.

qPCR

The sequences of the primers used are given in Supplemental Table S1. The cDNA samples were analyzed with the iCycler iQ System (Bio-Rad, USA). The qPCR reaction mixes contained 10 µl of Bio-Rad 1x iQ SYBR Green Supermix, 0.5 µM of each primer and 1 µl of cDNA for a 20 µl end volume reaction. The qPCR program started with a 3 min initial denaturation step at 95 ºC followed by 40 cycles of amplification (95 ºC for 10 s, 54 ºC for 15 s and 72 ºC for 30 s) with continuous monitoring of the SYBR Green fluorescence. The reaction ended with a melting curve step from 55 ºC to 95 ºC at 0.5 ºC per second. Data analysis was carried out with the Bio-Rad Optical System Software 5.0.

HPLC-ESI-MS/MS analysis

Methanolic extracts of lyophilized sorted cells were separated on an HPLC Accela (Thermo Fischer Scientific, Bremen, Germany) using a Phenomenex Gemini® C18 column (150 x 4.6 mm; 3 µm particle size). The mobile phase consisted of methanol (A) and 25 mM ammonium acetate pH 10.0 (B) mixed to form the following gradient: 40% B at 0 min, 38% B at 6 min, 38% B at 35 min, 25% B at 40 min, 10% B at 45 min, 40% B at 50 min, and 40% B at 55 min. Elution was performed with a flow rate of 0.5 mL min^{-1} and the injection volume

was 20 µL. MS analysis was performed on an LTQ OrbitrapTM XL hybrid mass spectrometer (Thermo Fischer Scientific, Bremen, Germany) controlled by LTQ Tune Plus 2.5.5 and Xcalibur 2.1.0. The electrospray ionization source settings (ESI) were: source voltage at 3.1 kV, capillary temperature at 275 ºC with a sheath gas flow rate of 40 and an auxiliary gas flow rate of 10 (arbitrary unit as provided by the software settings), capillary voltage at 48 V, and tube lens voltage at 115 V. The MS data handling software Xcalibur QualBrowser software, Thermo Fischer Scientific was used to search for predicted metabolite by their exact *m/z* value. All peaks were checked for *m/z* value and fragmentation products.

Accession numbers

Accession numbers in the database Cathacyc (http://www.cathacyc.org): *RPSL24* - Caros004968.2, *D4H* - Caros006133.1, *DAT* - Caros 016117.1.

Supplemental Data

The following materials are available in the online version of this article.

Supplemental Figure S1. General scheme of the *C. roseus* monoterpenoid indole alkaloid pathway leading to the anticancer alkaloids vinblastine and vincristine.

Supplemental Table S1. List of primers used in this work.

ACKNOWLEDGEMENTS

The authors would like to thank Pedro Lima (IGC) for the help with fluorescence and confocal microscopy, Paula Sampaio (IBMC) for the help with the preparation of figures, Filipe Borges (IGC) for the assistance during RNA extraction, Manuel Joaquim Bastos Marques (Dep Physics and Astronomy, FCUP) for helping with the interpretation of bright-field images, and Silvia Maia from Centro de Materiais da Universidade do Porto (CEMUP) for technical assistance with mass spectrometry.

FIGURE LEGENDS

Figure 1. Bright-field optical microscopy images of *C. roseus* whole leaves infiltrated with alkaloid indicators reveal a positive reaction in idioblasts (stained isolated mesophyll cells) and laticifers (stained threads). A to D, Infiltration with the reagent of Dragendorff reveals alkaloid accumulating cells stained in brown. E to H, Infiltration with the reagent of Mayer reveals alkaloid accumulating cells stained in dark grey. A, B, E and F, Images of the adaxial face. C, D, H, and H, Images of the abaxial face. Focusing of leaf images was performed based on the detection of stained cells, which appeared only below the epidermis cell layer. Bars = 200 µm (A, C, E and G) and 50 µm (B, D, F and H).

Figure 2. Epifluorescence microscopy images of *C. roseus* whole leaves. A, Image of the adaxial face. B, Image of the abaxial face. 1, Red channel revealing autofluorescence of chlorophyll in chloroplasts. 2, Blue channel revealing the presence of an autofluorescence signal in idioblasts. 3, Green channel revealing the presence of an autofluorescence signal in idioblasts. 4, Merged images of the three channels. Bars = 100 µm.

Figure 3. A, Bright-field image (A1) of *C. roseus* leaf protoplasts and the correspondent fluorescence image showing the viable protoplasts that incorporated and modified FDA to generate green fluorescence (A2). B, Bright-field image of protoplasts treated with the reagent of Dragendorff showing an idioblast with the vacuole content stained in brown. C, Bright-field image of protoplasts treated with the reagent of Mayer showing an idioblast with the vacuole content stained in dark grey (many protoplasts burst in the presence of this reagent). D, Bright-field image of protoplasts focused at the mid-plane (D1) and above the mid-plane (D2) showing an idioblast with a distinctive bright halo. E, Bright-field and epifluorescence microscopy images of leaf protoplasts with cells: focused at the mid plane (E1), focused above the mid plane showing that idioblasts display a distinctive bright halo (E2), observed with the blue channel revealing idioblast protoplasts (E3), observed with the green channel revealing idioblast protoplasts (E4), and represented by the merged image of E1, E3 and E4 (E5). Bars = 10 µm (A, B and D) and 20 µm (C and E).

Figure 4. Autofluorescence emission spectra of *C. roseus* mesophyll cells. A, Confocal (A1) and bright-field (A2) images of the adaxial face of a whole mounted leaf focused at the level of the palisade parenchyma. B, Confocal (B1) and bright-field (B2) images of the abaxial face of a whole mounted leaf focused at the level of the spongy parenchyma. C, Confocal (C1) and bright-field (C2) images of mesophyll protoplasts. D, Emission spectra of the cells indicated in A, B and C. upon excitation with a 405 nm laser. Bars = 50 µm (A and B) and 20 µm (C).

Figure 5. Dot plots obtained during sorting of *C. roseus* leaf protoplasts. A, Dot plot of red versus green emissions with indication of the two populations selected as common mesophyll cells (I) and idioblasts (II), based on bright field and fluorescence microscopy of the sorted cells (Fig. 6). Events corresponding to debris were excluded from the dot plot. B, Dot plots of forward scatter (FSC) vs. side scatter (SSC) of the two populations highlighted in A. Crosses indicate medians of populations in both FSC and SSC.

Figure 6. Epifluorescence microscopy images of a source C. roseus leaf protoplast suspension (A) and of populations of mesophyll cells (B and C) and idioblasts (D and E) isolated by FACS. 1, Red channel revealing autofluorescence of chlorophyll in chloroplasts. 2, Blue channel revealing the presence of an autofluorescence signal in idioblasts. 3, Green channel revealing the presence of an autofluorescence signal in idioblasts. 4, Merged images of the three channels. 5, Merge of the blue and green channel images with the correspondent bright-field image. Bars = 40 µm (A, B and D) and 5 µm (C and E).

Figure 7. Expression of *D4H* and *DAT* in sorted common mesophyll and idioblast protoplasts. Transcript levels were determined by qPCR and normalized using Cr*RPSL24* (p<0.05 for both genes, Student's t-test).

Figure 8. Base peak chromatogram of *m/z* 457.23 and respective MS fragment pattern. A, Vindoline standard (0.5 µg mL^{-1}). B, Sorted idioblast protoplasts (115 cells μL^{-1}). C, Sorted common mesophyll protoplasts (800 cells μL^{-1}).

484

485

Parsed Citations

Birnbaum K, Jung JW, Wang JY, Lambert GM, Hirst JA, Galbraith DW, Benfey PN (2005) Cell type-specific expression profiting in plants via cell sorting of protoplasts from fluorescent reporter lines. Nat Methods 2: 615-619
Pubmed: Author and Title
CrossRef: Author and Title
Google Scholar: Author Only Title Only Author and Title

Bruneton J (2009) Pharmacognosie: phytochimie, plantes médicinales. 4e édition, revue et augmentée. Lavoisier Tec & Doc, Paris
Pubmed: Author and Title
CrossRef: Author and Title
Google Scholar: Author Only Title Only Author and Title

Carqueijeiro I, Noronha H, Duarte P, Geros H, Sottomayor M (2013) Vacuolar transport of the medicinal alkaloids from Catharanthus roseus is mediated by a proton-driven antiport. Plant Physiol 162: 1486-1496
Pubmed: Author and Title
CrossRef: Author and Title
Google Scholar: Author Only Title Only Author and Title

Carter AD, Bonyadi R, Gifford ML (2013) The use of fluorescence-activated cell sorting in studying plant development and environmental responses. Int J Dev Biol 57: 545-552
Pubmed: Author and Title
CrossRef: Author and Title
Google Scholar: Author Only Title Only Author and Title

Courdavault V, Papon N, Clastre M, Giglioli-Guivarc'h N, St-Pierre B, Burlat V (2014) A look inside an alkaloid multisite plant: the Catharanthus logistics. Curr Opin Plant Biol 19: 43-50
Pubmed: Author and Title
CrossRef: Author and Title
Google Scholar: Author Only Title Only Author and Title

De Luca V, Salim V, Thamm A, Masada SA, Yu F (2014) Making iridoids/secoiridoids and monoterpenoid indole alkaloids: progress on pathway elucidation. Curr Opin Plant Biol 19: 35-42
Pubmed: Author and Title
CrossRef: Author and Title
Google Scholar: Author Only Title Only Author and Title

Fang J, Schneider B (2014) Laser microdissection: a sample preparation technique for plant micrometabolic profiling. Phytochem Anal 25: 307-313
Pubmed: Author and Title
CrossRef: Author and Title
Google Scholar: Author Only Title Only Author and Title

Galbraith D (2010) Flow cytometry and fluorescence-activated cell sorting in plants: the past, present, and future. Biomédica 30: 61-69
Pubmed: Author and Title
CrossRef: Author and Title
Google Scholar: Author Only Title Only Author and Title

Kellner F, Geu-Flores F, Sherden NH, Brown S, Foureau E, Courdavault V, O'Connor SE (2015) Discovery of a P450-catalyzed step in vindoline biosynthesis: a link between the aspidosperma and eburnamine alkaloids. Chem Commun 51: 7626-7628
Pubmed: Author and Title
CrossRef: Author and Title
Google Scholar: Author Only Title Only Author and Title

Mersey BG, Cutler AJ (1986) Differential distribution of specific indole alkaloids in leaves of Catharanthus roseus. Can J Bot 64: 1039-1045
Pubmed: Author and Title
CrossRef: Author and Title
Google Scholar: Author Only Title Only Author and Title

Miettinen K, Dong L, Navrot N, Schneider T, Burlat V, Pollier J, Woittiez L, van der Krol S, Lugan R, Ilc T, Verpoorte R, Oksman-Caldentey K-M, Martinoia E, Bouwmeester H, Goossens A, Memelink J, Werck-Reichhart D (2014) The seco-iridoid pathway from Catharanthus roseus. Nat Commun 5: 3606
Pubmed: Author and Title
CrossRef: Author and Title
Google Scholar: Author Only Title Only Author and Title

Murata J, De Luca V (2005) Localization of tabersonine 16-hydroxylase and 16-OH tabersonine-16-O-methyltransferase to leaf epidermal cells defines them as a major site of precursor biosynthesis in the vindoline pathway in Catharanthus roseus. Plant J 44: 581-594
Pubmed: Author and Title
CrossRef: Author and Title
Google Scholar: Author Only Title Only Author and Title

Renaudin JP (1985) Extraction and fluorimetric detection after high-performance liquid-chromatography of indole alkaloids from cultured-cells of Catharanthus roseus. Physiol Veg 23: 381-388
Pubmed: Author and Title
CrossRef: Author and Title

Google Scholar: Author Only Title Only Author and Title

St-Pierre B, Vazquez-Flota FA, De Luca V (1999) Multicellular compartmentation of Catharanthus roseus alkaloid biosynthesis predicts intercellular translocation of a pathway intermediate. Plant Cell 11: 887-900

Pubmed: Author and Title
CrossRef: Author and Title
Google Scholar: Author Only Title Only Author and Title

Stavrinides A, Tatsis EC, Foureau E, Caputi L, Kellner F, Courdavault V, O'Connor SE (2015) Unlocking the diversity of alkaloids in Catharanthus roseus: nuclear localization suggests metabolic channeling in secondary metabolism. Chem Biol 22: 336-341

Pubmed: Author and Title
CrossRef: Author and Title
Google Scholar: Author Only Title Only Author and Title

Yoder LR, Mahlberg PG (1976) Reactions of alkaloid and histochemical indicators in laticifers and specialized parenchyma cells of Catharanthus roseus (Apocynaceae). Amer J Bot 63: 1167-1173

Pubmed: Author and Title
CrossRef: Author and Title
Google Scholar: Author Only Title Only Author and Title

Yu F, De Luca V (2013) ATP-binding cassette transporter controls leaf surface secretion of anticancer drug components in Catharanthus roseus. Proc Natl Acad Sci USA 110: 15830-15835

Pubmed: Author and Title
CrossRef: Author and Title
Google Scholar: Author Only Title Only Author and Title